The main modes analysis of continuous curved box-girder bridge

Dai Fan[1] &He Jian[1] &You Shangyou[1] & Zhao Zhengjiiu[2]

[1]Zhanjiang City Highway Authority, Zhanjiang, Guangdong 524043, China

[2]College of Science and Engineering, Jinan University, Guangzhou, Guangdong 510000, China

[a]daifan666@163.com;jjk1206@126.com;[c]191493928@qq.com;zzj_jnu@163.com (corresponding author)

KEYWORD: radius of curvature; variable pre-stressed continuous curved box-girder bridge; main modes;

ABSTRACT: According the bridge，132 meters long tapered ，continuous curved box-girder bridge as the research object. Divide the continuous beam bridge models into vertical bending, pure torsion, lateral bending and longitudinal movement of the four sub-direction. Each energy of the vibration mode also divided into vertical bending energy, torsion energy, energy and transverse bending along the longitudinal direction of the translational energy of four energy. Introduce four directions coefficient to represent the energy of each sub-share each vibration direction, respectively the ratio type of energy, and to judge the main modes tapered continuous curved box-girder bridge.

Fund project: 2014 industry support research project, funded by Guangdong Province highway Administration. Project number: 2014-11,

Introduction

Main modes on the mass matrix and the stiffness matrix is the inherent property of orthogonal multi-degree of freedom systems. If up to the physical meaning of the orthogonality of the main modes possessed by the energy level from the study, potential energy and kinetic energy of the multi-degree of freedom system can be expressed as:

$$U = \frac{1}{2} y^T K y \qquad (1)$$

$$T = \frac{1}{2} \dot{y}^T M \dot{y} \qquad (2)$$

Assume that there are two main vibration system free vibration at the initial condition, there are:

$$y = A_{1i} f_i \sin(w_i t + a_i) + A_{1j} f_j \sin(w_j t + a_j) \quad (1)$$

Derivative of the above formula, then the speed is:

$$\dot{y} = A_{1i} w_i f_i \cos(w_i t + a_i) + A_{1j} w_j f_j \cos(w_j t + a_j) \quad (1)$$

The potential energy and the kinetic energy of the system can be expressed as:

$$U = \frac{1}{2} \{A_{1i} f_i \sin(w_i t + a_i) + A_{1j} f_j \sin(w_j t + a_j)\}^T \cdot K \cdot \{A_{1i} f_i \sin(w_i t + a_i) + A_{1j} f_j \sin(w_j t + a_j)\} \qquad (3)$$

$$T = \frac{1}{2} \{A_{1i} w_i f_i \cos(w_i t + a_i) + A_{1j} w_j f_j \cos(w_j t + a_j)\}^T \cdot M \cdot \{A_{1i} w_i f_i \cos(w_i t + a_i) + A_{1j} w_j f_j \cos(w_j t + a_j)\} \qquad (4)$$

By the main modes of orthogonality can be obtained:

$$U = \frac{1}{2} K_i A_{1i}^2 \sin^2(w_i t + a_i) + \frac{1}{2} K_j A_{1j}^2 \sin^2(w_j t + a_j) = U_i + U_j \qquad (5)$$

$$T=\frac{1}{2}M_iA_{1i}^2w_i^2\cos^2(w_it+a_i)+\frac{1}{2}M_jA_{1j}^2w_j^2\cos^2(w_jt+a_j) \quad (6)$$
$$=T_i+T_j$$

From the above equation, because the main orthogonal modes makes the system has two main modes under the circumstances, the potential energy or kinetic energy of the system are the two main modes alone are the kinetic and potential energy and or. And when

$$U_i+T_i=\frac{1}{2}K_iA_{1i}^2\sin^2(w_it+a_i)+\frac{1}{2}M_iA_{1i}^2w_i^2\cos^2(w_it+a_i) \quad (7)$$
$$=\frac{1}{2}M_iA_{1i}^2w_i^2$$

Main vibrations within the system can be transformed into potential energy and kinetic energy with each other, when the vibration of single degree of freedom system as independent as the main vibration energy between each order can not pass each other.

Four representatives of each of the above-defined modes direction parameters represent each vibration energy accounted for the proportion of each type of energy modes with sub-direction:

$$a_j=\sum_{i=1}^{n}(m_i\cdot u_{z_{ij}}^2)+\sum_{i=1}^{n}(J_{y_i}\cdot q_{y_{ij}}^2)/[\sum_{i=1}^{n}(m_i\cdot u_{z_{ij}}^2)+\sum_{i=1}^{n}(J_{y_i}\cdot q_{y_{ij}}^2)+\sum_{i=1}^{n}(J_{x_i}\cdot q_{x_{ij}}^2) \quad (8)$$
$$+\sum_{i=1}^{n}(m_i\cdot u_{y_{ij}}^2)+\sum_{i=1}^{n}(J_{z_i}\cdot q_{z_{ij}}^2)+\sum_{i=1}^{n}(m_i\cdot u_{x_{ij}}^2)]$$

$$b_j=\sum_{i=1}^{n}(J_{x_i}\cdot q_{x_{ij}}^2)/[\sum_{i=1}^{n}(m_i\cdot u_{z_{ij}}^2)+\sum_{i=1}^{n}(J_{y_i}\cdot q_{y_{ij}}^2)+\sum_{i=1}^{n}(J_{x_i}\cdot q_{x_{ij}}^2) \quad (9)$$
$$+\sum_{i=1}^{n}(m_i\cdot u_{y_{ij}}^2)+\sum_{i=1}^{n}(J_{z_i}\cdot q_{z_{ij}}^2)+\sum_{i=1}^{n}(m_i\cdot u_{x_{ij}}^2)]$$

$$g_j=\sum_{i=1}^{n}(m_i\cdot u_{y_{ij}}^2)+\sum_{i=1}^{n}(J_{z_i}\cdot q_{z_{ij}}^2)/[\sum_{i=1}^{n}(m_i\cdot u_{z_{ij}}^2)+\sum_{i=1}^{n}(J_{y_i}\cdot q_{y_{ij}}^2) \quad (10)$$
$$+\sum_{i=1}^{n}(J_{x_i}\cdot q_{x_{ij}}^2)+\sum_{i=1}^{n}(m_i\cdot u_{y_{ij}}^2)+\sum_{i=1}^{n}(J_{z_i}\cdot q_{z_{ij}}^2)+\sum_{i=1}^{n}(m_i\cdot u_{x_{ij}}^2)]$$

$$x_j=\sum_{i=1}^{n}(m_i\cdot u_{x_{ij}}^2)/[\sum_{i=1}^{n}(m_i\cdot u_{z_{ij}}^2)+\sum_{i=1}^{n}(J_{y_i}\cdot q_{y_{ij}}^2)+\sum_{i=1}^{n}(J_{x_i}\cdot q_{x_{ij}}^2) \quad (11)$$
$$+\sum_{i=1}^{n}(m_i\cdot u_{y_{ij}}^2)+\sum_{i=1}^{n}(J_{z_i}\cdot q_{z_{ij}}^2)+\sum_{i=1}^{n}(m_i\cdot u_{x_{ij}}^2)]$$

Seismic Response of curved continuous box-girder Bridge

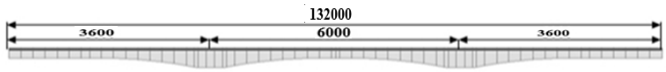

Fig.1 Developed View

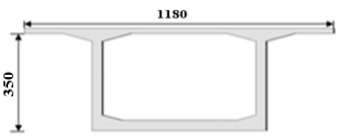

Fig.2 Support-Section of the box girder

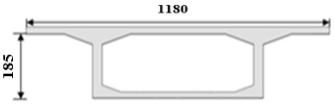

Fig.3 Cross-Section of the box girder

Bridge Description. The bridge is a total length of 132m three-span continuous pre-stressed concrete box-girder bridge. (Fig.1) Box-girder cross-section for the single-chamber single box, roof wide 11.8m, bottom width 6.8m, top and bottom of box-girder with the same slope. Both sides of the cantilever flange plate width 2.5m, the ends of the cantilever plate thickness of 15cm, the roots

of 60cm. Root box-girder beam height H = 3.5m, across the center of the beam height H = 1.85m, beam height changes via 2.0 times parabola. (Fig.2) (Fig.3)

Finite Element Models.

Creating the variable cross-section of pre-stressed curved box-girder bridge box-girder bridge models, straight or curved, with different radius of curvature in same span of 132m by using the finite element software Midas/Civil for analysis. Discuss the main mode of the bridge in vibration of the different radius of curvature in the allowable range. Definite the material of the main variable cross-section of pre-stressed continuous curved box-girder bridge beams as the C55 concrete, elastic modulus E = 3.55*MPa. According to materials and design section provided in Midas/Civil database, and due consideration to the upper section of the eccentric, the establishment of variable cross-section of different radii of curvature continuous prestressed curved box-girder bridge superstructure model. (Fig.4).

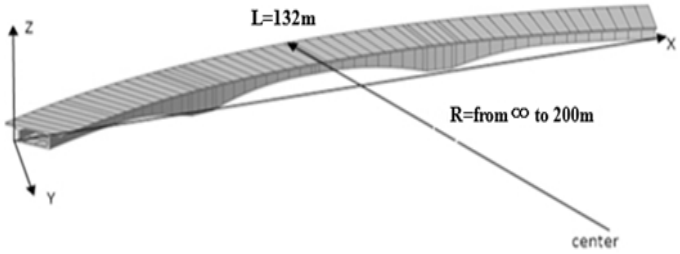

Fig.4 Finite element model (*R* is the radius of curvature)

Loads and boundary conditions.

The model simulated five kinds of loads: structural weight, cradle load, load prestressed concrete shrinkage and creep load, lane load. The above five kinds of loads, shrinkage and creep except in accordance with the procedures defined contraction function automatically calculates the creep, the other loads information must be defined. Weight of the bridges weight can be added with coefficients given by the Midas/Civil procedure; Cradle load can be simulated through the node load, Cradle role outside of 2.452m at the end of the cantilever, cradle translated load of 10KN and additional moment 24.52KNm; Prestressing loads can be added during the construction phase, loaded 1300N/mm ² of prestressing steel beam. Lane load was defined as asphalt road and designate wheel spacing 1.8m to simulate the vehicle or carrier in the form of a tube lane.

During the construction process, T structure should be the first part of the construction and the main beam consolidate with pier; After the closured of side-span was done, the system of mid-pier needs to be converted in order to change the side-span into the state of single cantilever; After the closured of mid-span was roped together, all of the bridge forming a three-span continuous system. Therefore, simulate the state of consolidation by a rigid connection of elastic consolidation and to simulate the state of system conversion by primary connection rigidity. Supports of side-span can be stimulated directly by movable hinge support.

Calculated Numerical Results.

Table1 Main mode and coupling mode of Xiaodongjiang Bridge (when R=400)

R=400				
Mode Number	α	β	γ	ξ
1	99.350%	0.007%	0.001%	0.642%
2	61.797%	0.014%	0.069%	38.120%
3	42.067%	0.009%	0.184%	57.740%
4	95.500%	0.018%	0.116%	4.365%
5	0.034%	0.819%	98.009%	1.138%
6	98.987%	0.013%	0.024%	0.976%
7	3.243%	4.556%	90.553%	1.647%
8	1.086%	3.845%	94.463%	0.606%
9	93.226%	0.320%	4.636%	1.819%
10	88.002%	0.043%	0.530%	11.425%
11	13.779%	1.089%	25.718%	59.414%
12	4.015%	3.621%	73.535%	18.829%
13	91.935%	0.048%	0.171%	7.845%
14	98.002%	0.015%	0.018%	1.965%
15	0.108%	11.462%	87.600%	0.830%

Table2 Main mode and coupling mode of Xiaodongjiang Bridge (when R=400)

R=400		
Mode Number	Main mode	Coupling mode
1	vertical bending	Vb&Lm
2	vertical bending	Vb&Lm
3	longitudinal movement	Vb&Lm
4	vertical bending	Vb&Lm
5	lateral bending	Lb&Lm
6	vertical bending	Vb&Lm
7	lateral bending	Lb&Pt
8	lateral bending	Vb&Pt
9	lateral bending	Lb&Lm
10	vertical bending	Vb&Lm
11	longitudinal movement	Lb&Lm
12	longitudinal movement	Lb&Lm
13	vertical bending	Vb&Lm
14	vertical bending	Vb&Lm
15	lateral bending	Lb&Lm

Draw the line chart of the main modes coefficient follows the radius of curvature changes in the state of ultimate limit.

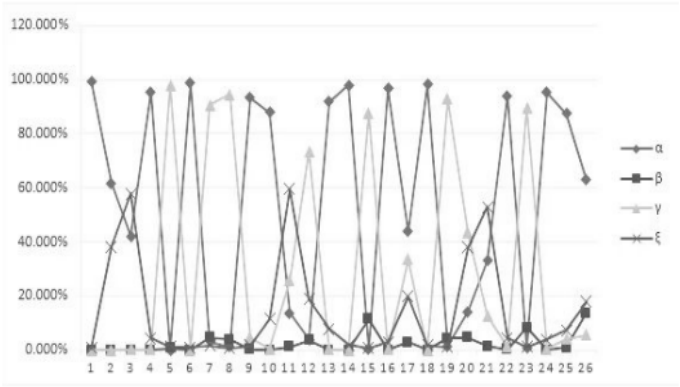

Fig.5 Main mode distribution map of the Xiaodongjiang bridge (when R=400)

As shown from the figure Xiaodongjiang bridge (ie, when R = 400), mainly to the vertical bending modes as well as the main negative lateral bending modes alternate with each other, while the main longitudinal translation of the previous modes 26 order of the main modes only appeared three times. The main disadvantage to reverse modes did not appear, but in the form of bending and torsion coupling consecutive first appeared in the 7th and 8th in vibration mode. From the entire modal distribution, with vertical bending modes still dominated the first of 26 vibration modes by occupy half of all. Analysis results for modal analysis radius of curvature of the curved bridge 400m in vertical bending remain as its most major modes. But should not be overlooked as one of the negative modes to lateral bending modes dominated the first 26 vibration mode accounted for one-third, but there is also based on a lateral bending vibration mode in the 8th bending and torsion coupling vibration mode, which makes the curved girder bridge had to face the adverse effects of vibration coupling between the two modes of the negative self-generated, especially in the curved girder bridge under the " cross-sectional design of axial symmetrical " situation.ever use letter spacing and never use more than one space after each other.

Draw the line chart of the vertical bending directions coefficient follows the radius of curvature changes.

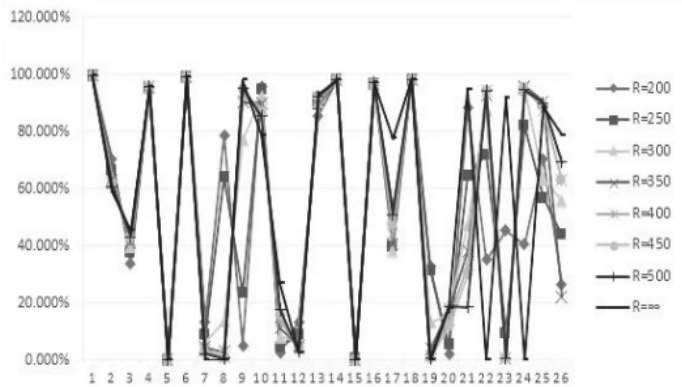

Fig.6 Vertical bending directions coefficient distribution map (from ∞ to 200)

From the above chart we can see that with the change of the radius of curvature, the first 26 to vertical vibration mode bending dominated modes still accounted for half, and the first six bands with vertical bending-dominated modes, the line vertical bending mode shape factor proportion of girder bridges are curved girder bridges other than the radius of curvature is large.

Draw the line chart of the pure torsion directions coefficient follows the radius of curvature changes .

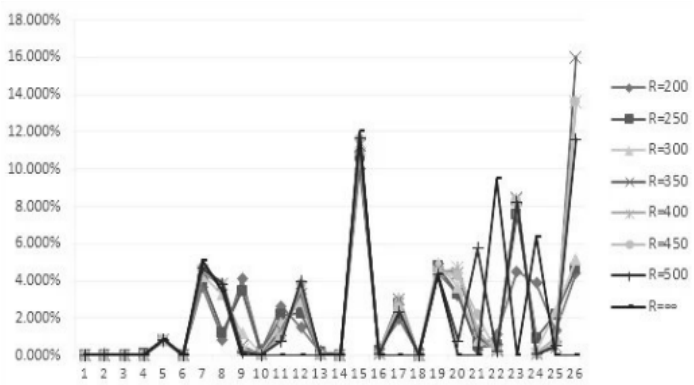

Fig.7 Pure torsion directions coefficient of different (from ∞ to 200)

As the above chart shows, the first seven modes in order to reverse the modal share of the main and not because of changes in the radius of curvature of the curved beam bridge produce much change. But in the 9-13 vibration modes 16-22 each vibration mode can be seen bearing the decreasing radius of curvature, reversing direction modal factor β gradually increasing trend. Although the reverse direction modal factor β in value more than other modes can't be the main factor modal direction, but as curved bridge modes unfavorable one, this change of trend is still worth a high degree of attention, especially in the use of " cross-sectional design of axial symmetrical "design method.

Draw the line chart of the torque follows the radius of curvature changes.

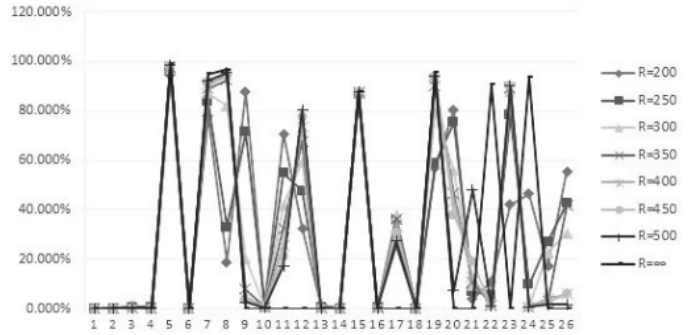

Fig.8 lateral bending directions coefficient of different (from ∞ to 200)

From the above chart shows, lateral bending direction of the linear beam bridge with a different radius curve factor Bridges previous eight vibration modes are basically the same size. However, the order of 9 to 13-order transverse direction of curvature factor of each radius of curvature with decreasing radius of curvature increases, and the transverse beam of linearly bending direction at this time the magnitude of the factor zero. With the emergence of the radius of curvature, lateral bending frequency-based modes appear in the previous 26-order modes in more and more.

Draw the line chart of the torque follows the radius of curvature changes.

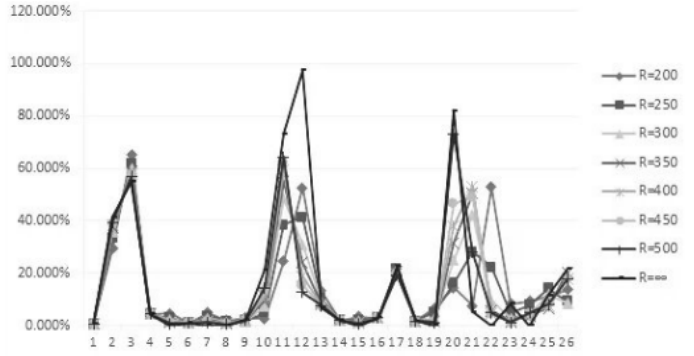

Fig.9 longitudinal translation directions coefficient of different (from ∞ to 200)

From the above chart shows, in longitudinal translation based on modal distribution, the distribution of the linear beam bridge with a radius of curvature of the bridge in roughly equal. But in the earlier onset of 11-13 vibration mode, the linear coefficient of beam bridge vertical shift direction are greater than the radius of curvature of each curved girder bridges.

Conclusions.

With the variation of curvature radius, pre-stressed continuous box-girder bridge vibration type direction coefficient has not big wave. Effect of curvature radius on the vibration type direction coefficient is small. In addition, there is no vibration or forward coupled vibration mode changes. With the radius of curvature decreases, each figure of the mode of main direction changes. As the unfavorable modes of pre-stress continuous box-girder bridge, the factor of torsional vibration and bending vibration has the tendency of raise in the first few modes. Especially when R=200 and R=250, transverse bending vibration appeared in advance in the ninth to eleventh order, and in the most unfavorable coupled vibration modes (transverse bending and torsion) appeared in the seventh order at earlier.

References.

[1] Xin.S.L,Ye.J.S,Yu.B S:Journal of Highway and Transportation Research and Development Vol.27(2010), p.79.
[2] Zheng.Y,Q:Journal of China & Foreign Highway Vol.33(2013), p.205.
[3] Chen.Z.L, Zhang.F: China Water Transport Vol.13(2013), p.299.
[4] Jing.G.Y: Shanxi Architecture Vol.39(2013), p.222.
[5] Gong.J.X,Zhao.G.F: China Civil Engineering Journal Vol.38(2005), p.1.
[6] Shu.W.X,Fang.S.P,Wu.L:Shanxi Architecturehina Vol.34(2008), p.315.
[7] Zhang.J: Shanxi Architecturehina Vol.37(2011), p.315.
[8] Zhou.X: Central South Highway Vol.28(2003), p.106.
[9] Hu.F.L: Engineering and Construction Vol.26(2012), p.366.